Supplemental Material

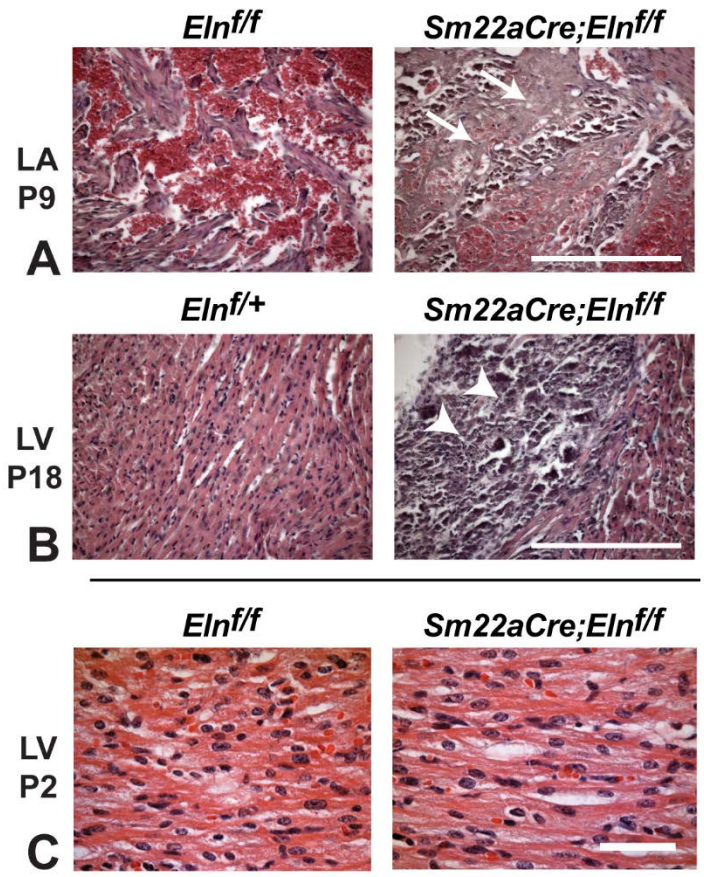

Online Figure I. Cardiac histopathology develops postnatally in mice with homozygous deletion of *Eln* in SMCs. (A) H&E staining reveals chronic thrombosis and calcification in the left atrium at P9 (arrows) and (B) necrosis and calcification in the left ventricle at P18 (arrowheads) in *Sm22aCre;Eln*$^{f/f}$ mice. (C) The myocardium of the left ventricle appears normal at P2. Scale bars = 100 μm.

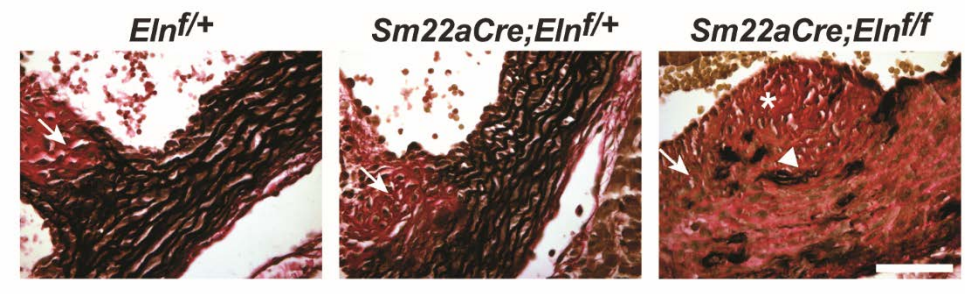

Online Figure II. Elastic laminae defects of the aortic root in mice with SMC deletion of *Eln*. VVG staining of the aortic root in *Sm22aCre;Eln*$^{f/f}$ mice looks similar to the ascending aorta (Fig. 4A) with a fragmented lEL (arrowhead) and neointimal formation (*). The connection to the aortic valve is marked with an arrow in each image. Scale bar = 50 μm.

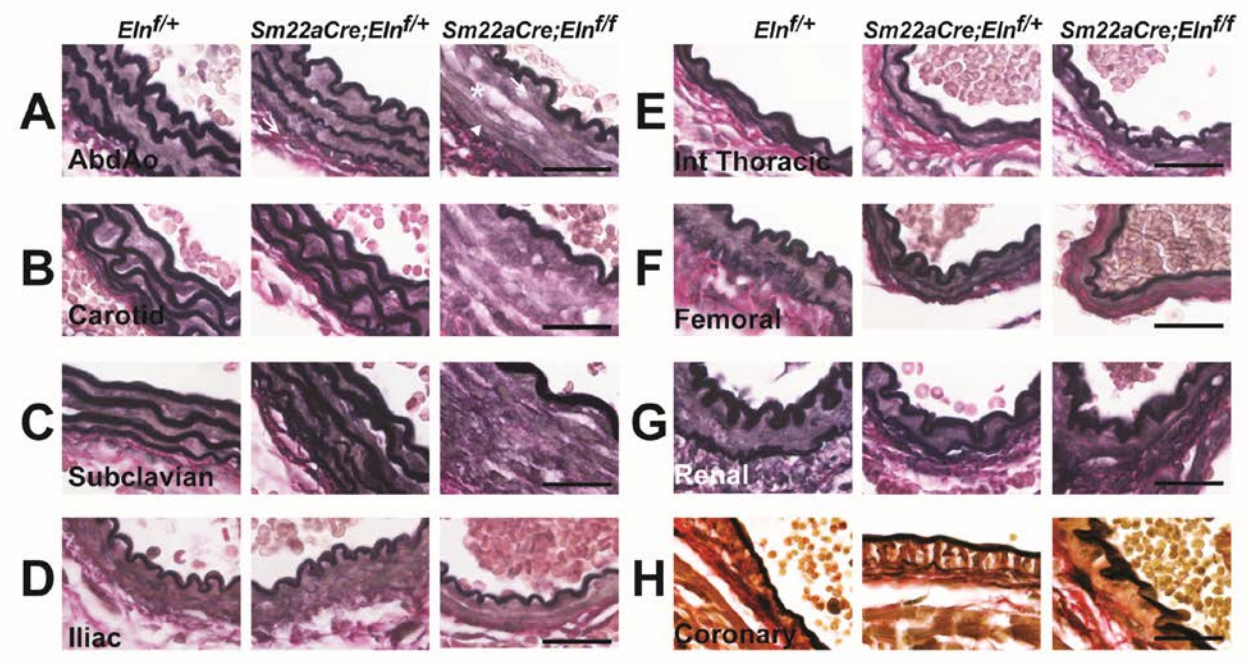

Online Figure III. VVG staining of multiple arteries in P8 mice with SMC deletion of *Eln* to evaluate IEL defects. The elastic arteries, including the abdominal aorta (A), carotid (B), and subclavian (C) look similar to the descending aorta (Fig. 4A) with an intact IEL. The IEL is also intact in the muscular/resistance arteries including the iliac (D), internal thoracic (E), femoral (F), renal (G), and coronary (H). Note that medial elastic lamellae are missing in *Sm22aCre;Eln*$^{f/f}$ arteries. Scale bars = 25 μm.

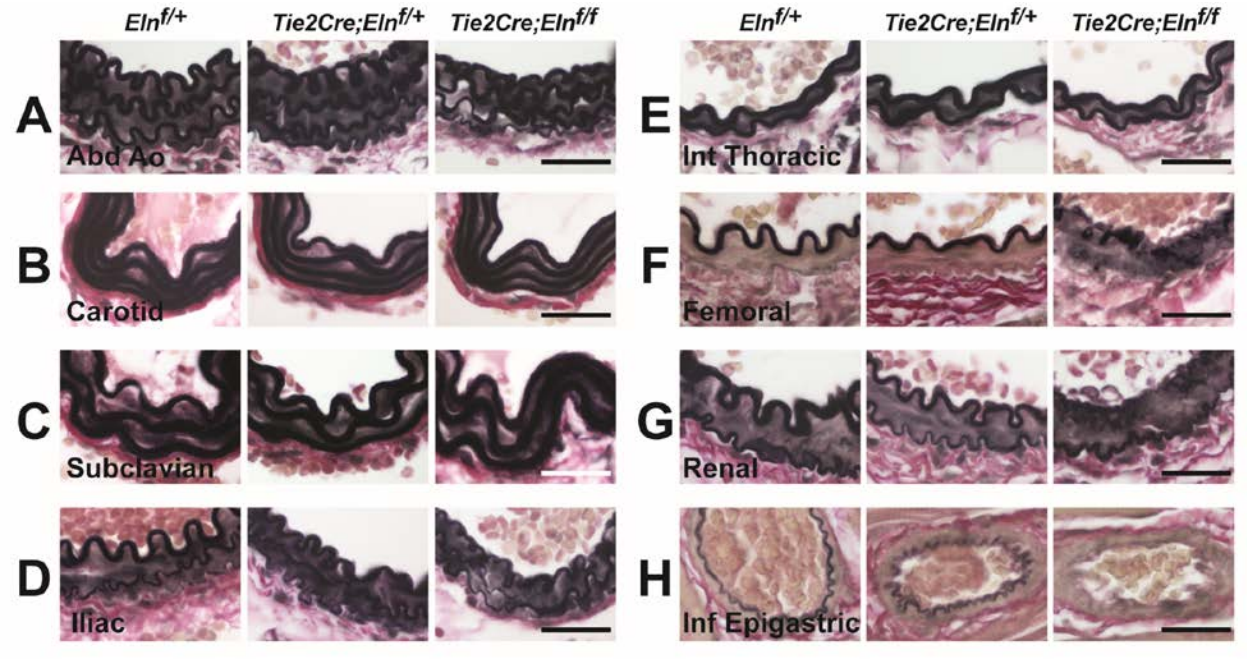

Online Figure IV. VVG staining of P10 arteries shows that EC deletion of *Eln* affects the IEL in muscular/resistance arteries. The IEL is intact in the abdominal aorta (A), carotid (B), subclavian (C), iliac (D), and internal thoracic (E) arteries, while it appears disrupted in the femoral (F) and renal (G) arteries and barely detectable in the inferior epigastric artery (H). Scale bars = 25 μm.